Geophysical Research Letters

Key Points:
- Conventional parametric relationships between radar reflectivity Z and rain rate R are not sufficient to capture precipitation variabilities
- A hybrid deep neural network system is designed for improved space radar rainfall estimation

Supporting Information:
- Supporting Information S1

Correspondence to:
H. Chen,
haonan.chen@noaa.gov

Rainfall Estimation From Ground Radar and TRMM Precipitation Radar Using Hybrid Deep Neural Networks

Haonan Chen[1,2] (iD), V. Chandrasekar[1], Haiming Tan[1], and Robert Cifelli[2]

[1]Department of Electrical and Computer Engineering, Colorado State University, Fort Collins, CO, USA, [2]NOAA/Earth System Research Laboratory, Boulder, CO, USA

Abstract Remote sensing of precipitation is critical for regional, continental, and global water and climate research. This study develops a deep learning mechanism to link between point-wise rain gauge measurements, ground-based, and spaceborne radar reflectivity observations. Two neural network models are designed to construct a hybrid rainfall system, where the ground radar is used to bridge the scale gaps between rain gauge and satellite. The first model is trained for ground radar using rain gauge data as target labels, whereas the second model is for spaceborne Tropical Rainfall Measuring Mission (TRMM) Precipitation Radar (PR) using ground radar estimates as training labels. Data from 1 year of observations in Florida during 2009 are utilized to illustrate the application of this hybrid rainfall system. Validation using independent data in 2009, as well as 2-year comparison against the standard PR products, demonstrates the promising performance and generality of this innovative rainfall algorithm.

Plain Language Summary The Tropical Rainfall Measuring Mission (TRMM) Precipitation Radar (PR) was the first spaceborne active sensor for observing precipitation over the tropics and subtropics. During its 17 years (1997–2014) in orbit and beyond, PR has been an important tool to characterize tropical precipitation microphysics and quantify rainfall rate over the globe. Ground validation is a critical component in the development of TRMM products. However, the ground-based sensors have different characteristics from PR in terms of resolution, viewing angle, and uncertainties in the sensing environments, which are not taken into account in the operational parametric rainfall relations applied to PR measurements. This study develops a nonparametric machine learning technique for PR rainfall estimation. In the regions where substantial gauge and ground radar data are available, this approach can produce better rainfall estimates compared to the standard PR algorithm. In areas such as ocean and remote regions where no gauge or radar available, the proposed rainfall algorithm is easy to implement, and it can still produce reasonable estimates. With more and more gauges and radars being deployed and many of them become operational, this algorithm can be trained at different locations represented by different atmosphere properties to further improve the performance and generality.

1. Introduction

Spaceborne and ground-based radars are efficient tools for observing precipitation and its 3-D microphysical structure. In principle, the functional relation between rain rate on the ground and the four-dimensional radar observations aloft can be obtained from measurements. However, it is difficult to express this functional relation in a simple form due to the complex space time variability in precipitation microphysics (Cifelli et al., 2018; Gou et al., 2018). The performance of radar-derived quantitative precipitation estimation greatly relies on the physical model of the raindrop size distribution (DSD) and the relation between the physical model and radar parameters (Bringi & Chandrasekar, 2001; Dolan et al., 2018; Wen et al., 2018). Conventional parametric relationships between radar reflectivity Z and rain rate R (so-called $Z - R$ relations) are not sufficient to capture such variabilities (Chen et al., 2017; Kirstetter et al., 2015; Kitchen et al., 1994; Steiner & Smith, 2000).

The Tropical Rainfall Measuring Mission (TRMM) satellite was launched in 1997 to observe moderate to heavy rainfall over the tropical and subtropical regions (Kummerow et al., 1998). Since then, the TRMM satellite has collected substantial measurements through the world's first spaceborne Precipitation Radar (PR) to improve our understanding of the distribution of precipitation. The TRMM PR (Kozu et al., 2001)

is a unique instrument capable of resolving high-resolution vertical profiles of precipitation on local-to-global scale. However, fundamental challenges exist in performing PR algorithm development and product validation with ground observations. Spatially, the horizontal resolution of PR is about 4.5 km, much coarser compared to the point-wise surface weather stations. Temporally, available data pairs for comparison between PR and rain gauge measurements are scarce during a single precipitation event due to TRMM's limited coincident overpasses. It is impractical to deploy dense gauge networks over a very broad range in order to capture TRMM satellite footprints. In contrast to rain gauges, ground radars measure rainfall over large spatial extent from which one can obtain a large amount of coincident samples with PR. At the same time, ground radar can collect simultaneous observations with rain gauge networks in the temporal dimension.

Prior research has shown that neural networks can be used to estimate surface rainfall from ground radar measurements (Liu et al., 2001; Orlandini & Morlini, 2000; Xiao & Chandrasekar, 1997). This nonparametric approach can explore the complex functional relation from high dimension input space (i.e., radar data) to the target space (i.e., rain gauge measurements). However, the utilization of neural networks in rainfall estimation is subject to many factors such as the representativeness and sufficiency of the training data set and the generalization capability of the trained model to new data containing subseasonal-to-seasonal changes in precipitation (Teschl et al., 2007; Xu & Chandrasekar, 2005). This study builds an adaptive deep neural network system for TRMM PR rainfall estimation using rain gauge data as ground truth. Therein, we use ground radar to bridge the scale gaps between PR and rain gauges. This research is also motivated by the rapid development of deep learning techniques, which have been successfully implemented in many applications (LeCun et al., 2015).

In particular, two multi-layer perceptron (MLP) models are designed to form the hybrid rainfall system (Figure 1). First, a ground radar-based model (MLP-1) is trained using rain gauge measurements as target labels. The trained MLP-1 model is applied to derive ground radar rainfall estimates that will be used to train PR observations for space-based rainfall estimation. For the MLP-1 model, it is easy to obtain a large number of training data pairs since ground radar is able to scan over the same location covered by gauge networks in fine temporal resolution, which is not possible for PR. Then, the alignment approach described in Bolen and Chandrasekar (2003) is applied to match PR and ground radar observations for subsequent training of the MLP-2 model. Overall, the ground radar observations and products serve as a critical relay linking rain gauge measurements on the ground and PR observations from space.

2. Data Set and Methodology

2.1. Data Set

Ground radar and rain gauge data collected near Melbourne, FL, in the year 2009 are used to demonstrate the proposed hybrid system. In particular, ground radar reflectivity measurements within 100 km of the KMLB Weather Surveillance Radar - 1988 Doppler (WSR-88D) are considered. As shown in Figure 1c, the Constant Altitude Plan Position Indicator (CAPPI) reflectivity profiles are generated at 1-, 2-, 3-, and 4-km heights with 1-km horizontal resolution. Three rain gauge networks around the KMLB radar are utilized, including the Kennedy Space Center (KSC), South Florida Water Management District (SFL), and St. Johns Water Management District (STJ) data sets, which respectively contain 33, 46, and 99 stations. All the stations are managed and maintained by the National Aeronautics and Space Administration (NASA) Precipitation Measurement Mission (PMM) ground validation program (Wolff et al., 2005).

TRMM PR data from 542 coincident overpasses over Melbourne region during 2009 are collected, among which 74 cases have decent precipitation in both PR and KMLB radar observations and are used to train and test the MLP-2 model. PR data collected in other regions during 2009, as well as the data collected during 2013, are also used to demonstrate and evaluate the applicability of the hybrid rainfall system. In addition, the standard PR products derived by NASA and Japan Aerospace Exploration Agency (JAXA) are utilized to further demonstrate the feasibility of the proposed rainfall approach.

2.2. Methodology

Figure 1a illustrates the overall architecture of the hybrid rainfall algorithm. There are four main modules, namely: (1) the MLP-1 model linking rain gauges and ground radar, (2) alignment between ground radar
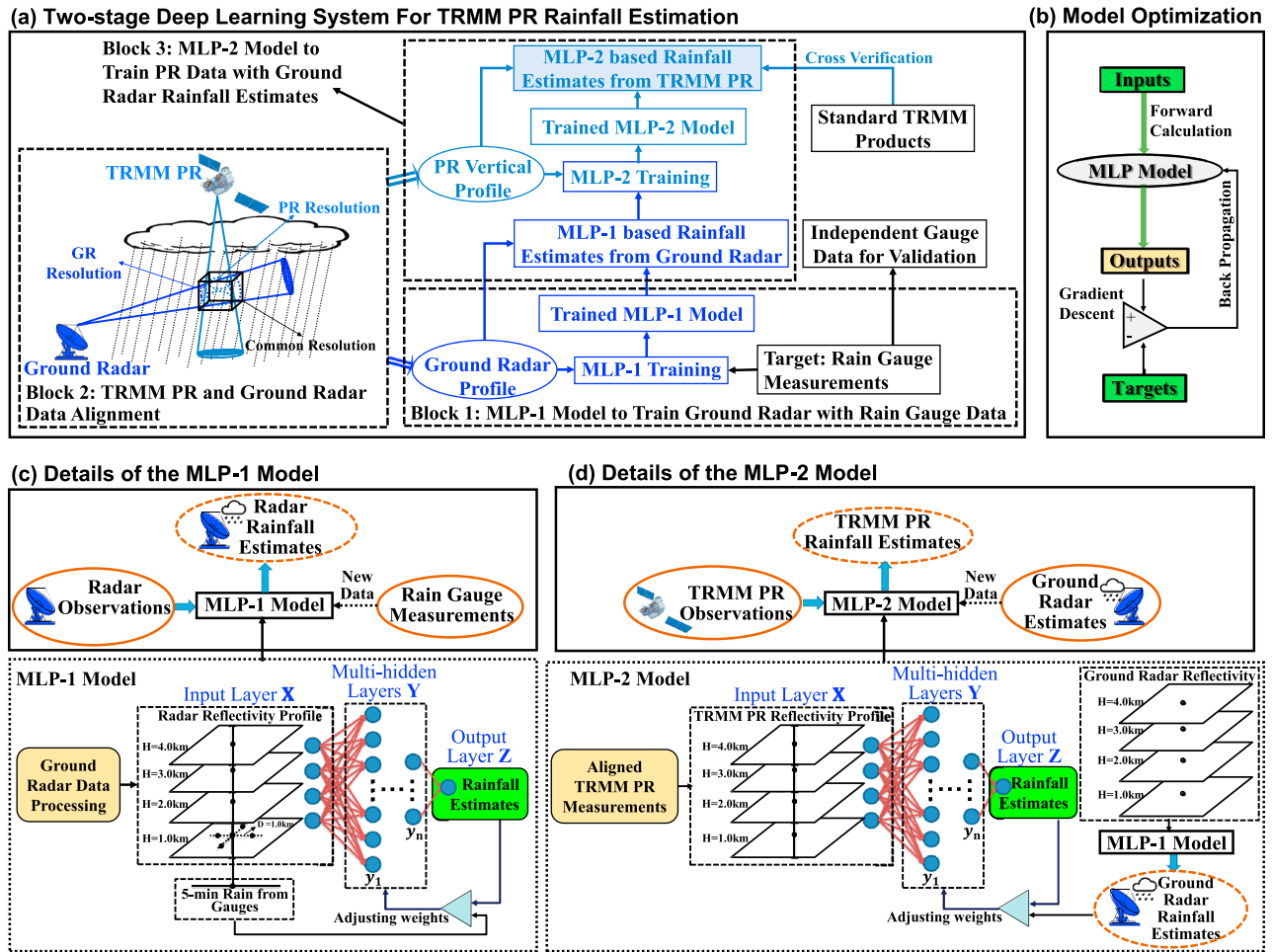
Figure 1. Two-stage deep learning system for Tropical Rainfall Measuring Mission (TRMM) Precipitation Radar (PR) rainfall estimation: (a) overall system diagram; Block 1 shows the conceptual diagram of the MLP-1 model designed for ground radar using rain gauge as target labels; Block 2 illustrates the geometry and alignment between ground-based and spaceborne radar measurements; Block 3 sketches the MLP-2 model for PR using ground radar rainfall estimates (from MLP-1) as target labels; (b) MLP model optimization for a predefined hyperparameter; (c) details of the MLP-1 model; (d) details of the MLP-2 model.

and PR measurements, (3) the MLP-2 model linking ground radar and PR, and (4) model and application product verification. Details of the MLP-1 and MLP-2 models are respectively shown in Figures 1c and 1d.

2.2.1. MLP-1 Model Design for Ground Radar Rainfall Estimation

As shown in Figures 1a and 1c, the MLP-1 model is constructed to estimate rainfall using ground radar observations. The system equation can be expressed in a general form as:

$$\mathbf{y_1} = f(\mathbf{w}_1\mathbf{X} + \mathbf{b}_1) \tag{1a}$$
$$\vdots$$
$$\mathbf{y_n} = f(\mathbf{w}_n\mathbf{y_{n-1}} + \mathbf{b}_n) \tag{1b}$$
$$\mathbf{Z} = f(\mathbf{w}_{n+1}\mathbf{y_n} + \mathbf{b}_{n+1}) \tag{1c}$$

where $\mathbf{X}$ is the input variable consisting of ground radar reflectivity profiles at four vertical levels (i.e., 1-, 2-, 3-, and 4-km height), $\mathbf{y_1}\cdots\mathbf{y_n}$ are the outputs of hidden layers from left to right, $\mathbf{w}_1$ is the weight vector for the input profiles, and $\mathbf{w}_2\cdots\mathbf{w}_{n+1}$ are the weights of the n hidden layer outputs, respectively; $\mathbf{b}_1\cdots\mathbf{b}_{n+1}$ are the bias terms associated with the input and hidden layers; $\mathbf{Z}$ is the output (i.e., ground radar rainfall estimates) that will be compared with the target labels (i.e., gauge measured rainfall).

AGU
100
ADVANCING EARTH
AND SPACE SCIENCE

Geophysical Research Letters

10.1029/2019GL084771

Similar to many other machine learning problems, it is not easy to predefine the model hyperparameters, including the number of hidden layers, the number of neurons/nodes for each layer, and the learning rate (Bergstra et al., 2011; Hinton & Salakhutdinov, 2006). The determination of hyperparameters for robust and accurate precipitation estimation for a given set of rain gauge, ground radar, and space radar data partly relies on our experience and experiments. In particular, a grid search approach is applied and many different hyperparameter candidates are tested in the training process to discover the one that results in the most accurate estimates. For each hyperparameter, the MLP model is optimized using the gradient descent algorithm (Burges et al., 2005). Figure 1b details the three-step optimization procedure, including forward propagation for estimation and the backward propagation to update the weights: (1) computation of the hidden layer outputs $\mathbf{y}_i$ and precipitation estimates $\mathbf{Z}$, (2) calculation of the cost function E of $\mathbf{Z}$ using target labels (gauge observations for MLP-1), and (3) error backward propagation to update weights $w_{i,j}$ based on the gradient $\frac{\partial E}{\partial w_{i,j}}$ until an optimal solution is reached. Here, the cost function E is defined as the mean square error of ground radar estimated rainfall RR_E with respect to rain gauge measurements RR_T:

$$E = \frac{1}{N} \sum (RR_E - RR_T)^2 \tag{2a}$$

$$w_{i,j(\text{new})} = w_{i,j(\text{old})} - \rho \frac{\partial E}{\partial w_{i,j(\text{old})}} \tag{2b}$$

where N is the total number of sample pairs, ρ is the learning rate of the MLP model, and $w_{i,j}$ is the weight associated with the jth node of the ith layer. It should be noted that the scale mismatch between gauge and ground radar is neglected in this study. That is, the point-wise gauge data are assumed to represent the 1-km by 1-km "areal" radar grid pixels. Temporally, 5-min scale is adopted in the MLP-1 model since the radar volume scan is updated every ~5 min. The 5-min rainfall estimates from radar and gauges are aggregated to hourly scale in the quantitative evaluation analysis.

In this study, the model is trained adaptively with the weights updated on a daily basis in order to capture the variations and avoid the propagation of uncertainties in larger temporal (e.g., monthly) scales (Liu et al., 2001; Tan et al., 2017). That is, the model is revised every day so as to include the newly available rain gauge and corresponding radar measurements. In total, 390,960 gauge 5-min rainfall samples and corresponding radar reflectivity profiles are utilized to train and test the MLP-1 model. The sample pairs are randomly split into training (80%) and testing (20%) subsets.

2.2.2. Alignment of TRMM-PR and Ground Radar Observations

The novelty of this deep learning system lies in the development of a link between rain gauges, ground, and space radars that sample precipitation from completely different geometrical aspects. Block 2 in Figure 1a shows the sampling differences between space and ground radar, where PR has a horizontal resolution of ~4.5 km but fine vertical resolution while ground radar has finer radial resolution (i.e., horizontal range) but varying vertical resolution depending on the distance from the radar. These two data sets need to be aligned in order to proceed with the MLP-2 model and subsequently derive rainfall products using PR measurements. To this end, the alignment approach developed by Bolen and Chandrasekar (2003) is used, which takes into account the differences in viewing angles, propagation paths, frequencies, resolution volume size, and time synchronization mismatch between space- and ground-based observations, as well as the geometric distortions caused by the movements and attitude perturbations of the spacecraft (see also Schwaller & Morris, 2011). In this process, both the ground-based and spaceborne radar data are resampled to a common grid so that direct comparison can be made between the two systems.

2.2.3. MLP-2 Model Design for TRMM PR Rainfall Estimation

Block 3 in Figure 1a sketches the MLP-2 model designed for PR. The manipulation process of the MLP-2 model is similar to MLP-1 in terms of the neural network structure and model optimization. Instead, the MLP-2 model takes the vertical profiles of PR reflectivity between 1 and 4 km as inputs. The corresponding target labels are rainfall estimates derived from the aligned ground radar observations using the trained MLP-1 model. In addition, the cost function E is defined as the mean square error of PR estimated rainfall rates with respect to ground radar rainfall rates.

It should be noted that the MLP-1 model is trained for all available precipitation events, whereas the MLP-2 model is trained only using coincident satellite overpasses and is updated only when a precipitating overpass
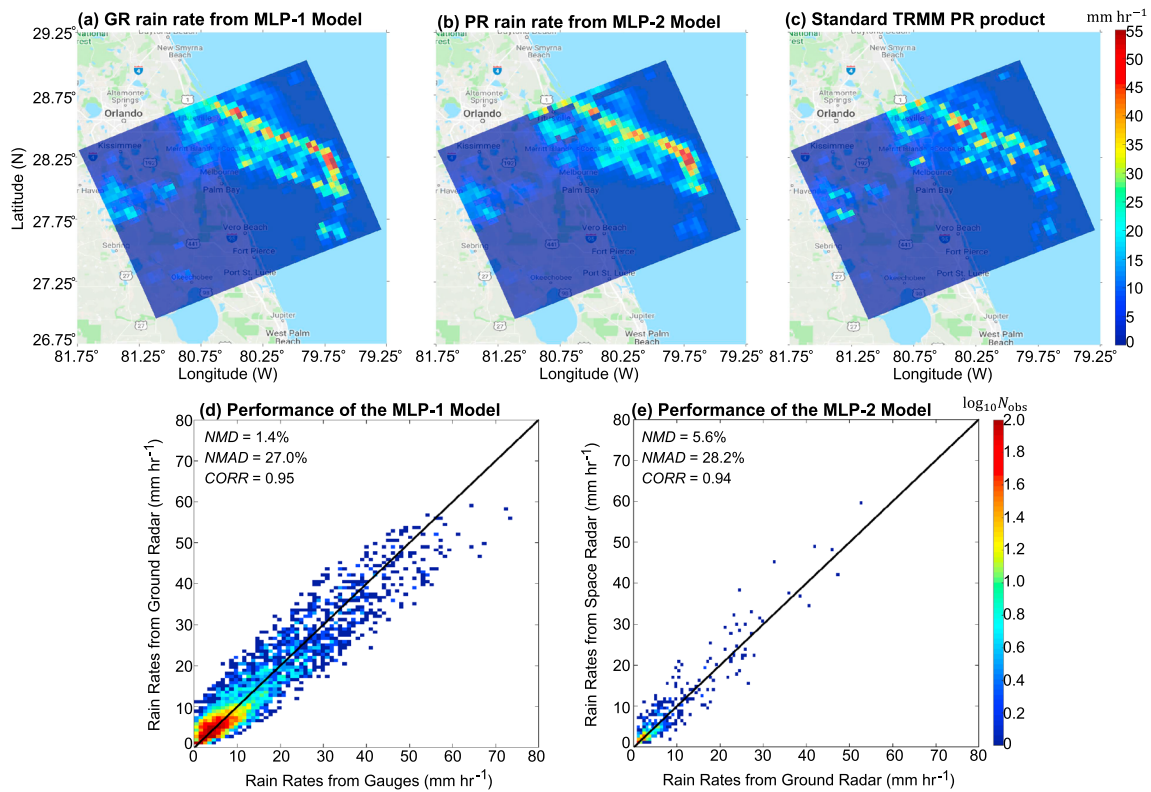
Figure 2. (a–c) Sample rainfall rate estimates from ground-based KMLB radar and spaceborne Tropical Rainfall Measuring Mission (TRMM) Precipitation Radar (PR) on 20 May 2009, at 0337UTC (satellite orbit #65574): (a) ground radar estimates using the MLP-1 model; (b) space radar estimates using the MLP-2 model; (c) standard TRMM PR product. (d and e) Model performance assessment using independent validation data in 2009: (d) ground radar rainfall estimates versus rain gauge measurements at hourly scale; (e) TRMM PR rainfall estimates versus ground radar product.

occurs. During the selected 74 overpass cases, there are 118,400 ground radar and PR sample pairs, among which 80% of the data are using for training and 20% are using for test.

2.2.4. Model and Product Validation

In order to demonstrate and evaluate this innovative approach for regional and global rainfall mapping, this letter compares the rain rate estimates from both MLP-1 and MLP-2 models with independent validation data set for the year 2009. In particular, for verification of the MLP-1 model, the testing data (20% of total sample pairs) of ground radar and gauges are used. For verification of the MLP-2 model, rainfall estimates derived from PR testing data (20% of total overpass samples) are compared with corresponding ground radar estimates. In addition, PR data collected for the whole year of 2013 are used to derive rainfall products to further verify the trained MLP-2 model. Regional and global rainfall maps at monthly and yearly scales are generated for PR using the trained MLP-2 model, and the rainfall maps are compared to the standard PR products from TRMM program to demonstrate the generic applicability of this novel rainfall system.

The following scoring metrics, including normalized mean difference (NMD), normalized mean absolute difference (NMAD), and Pearson correlation coefficient (CORR), are computed for quantitative assessment of the two MLP models as well as the derived PR product:

$$\mathrm{NMD} = \frac{\langle R_{\mathrm{Est}} - R_{\mathrm{Ref}} \rangle}{\langle R_{\mathrm{Ref}} \rangle} \tag{3a}$$

$$\mathrm{NMAD} = \frac{\langle |R_{\mathrm{Est}} - R_{\mathrm{Ref}}| \rangle}{\langle R_{\mathrm{Ref}} \rangle} \tag{3b}$$

$$\mathrm{CORR} = \frac{\sum [(R_{\mathrm{Est}} - \langle R_{\mathrm{Est}} \rangle)(R_{\mathrm{Ref}} - \langle R_{\mathrm{Ref}} \rangle)]}{\sqrt{\sum (R_{\mathrm{Est}} - \langle R_{\mathrm{Est}} \rangle)^2} \sqrt{\sum (R_{\mathrm{Ref}} - \langle R_{\mathrm{Ref}} \rangle)^2}} \tag{3c}$$
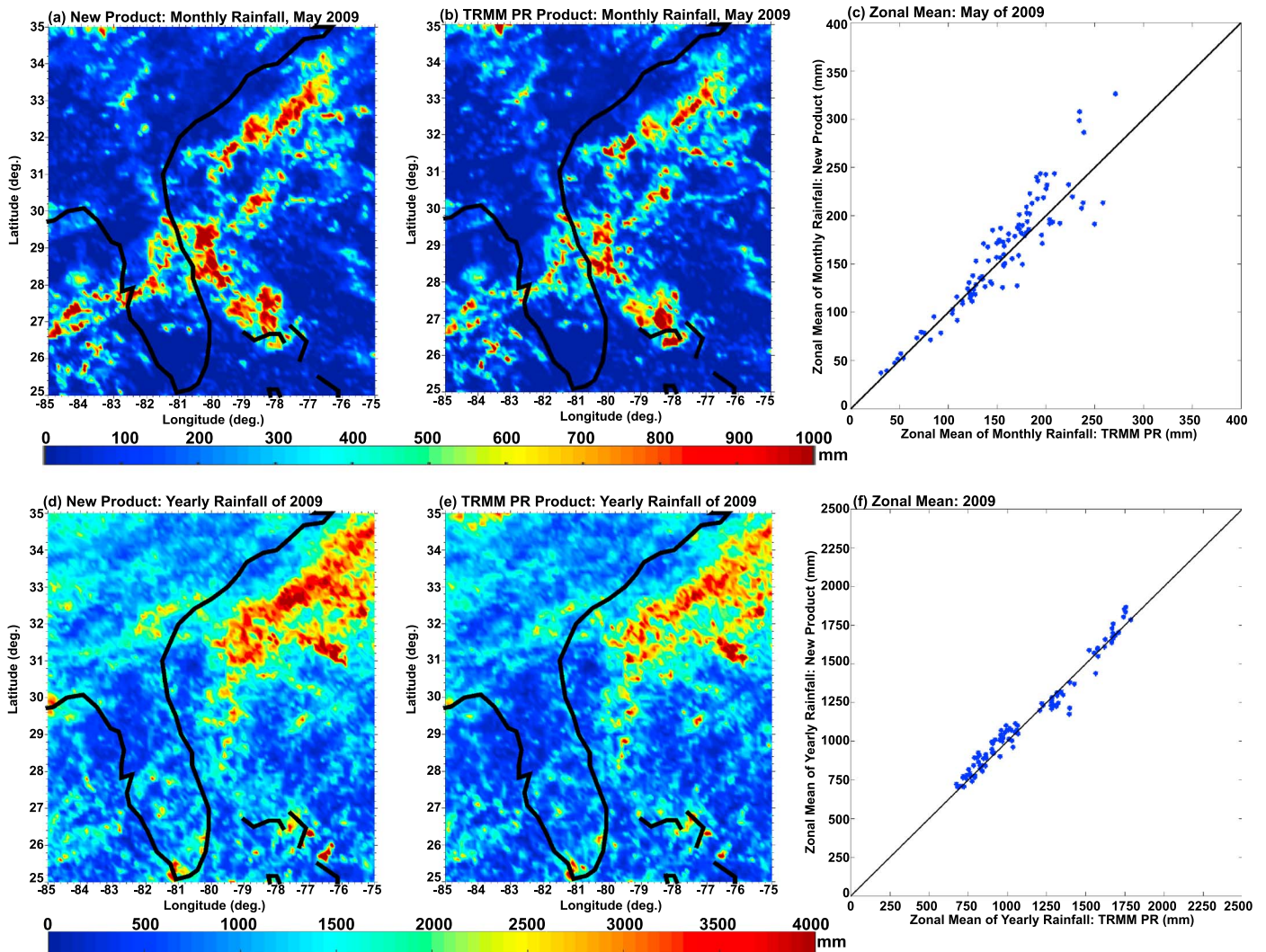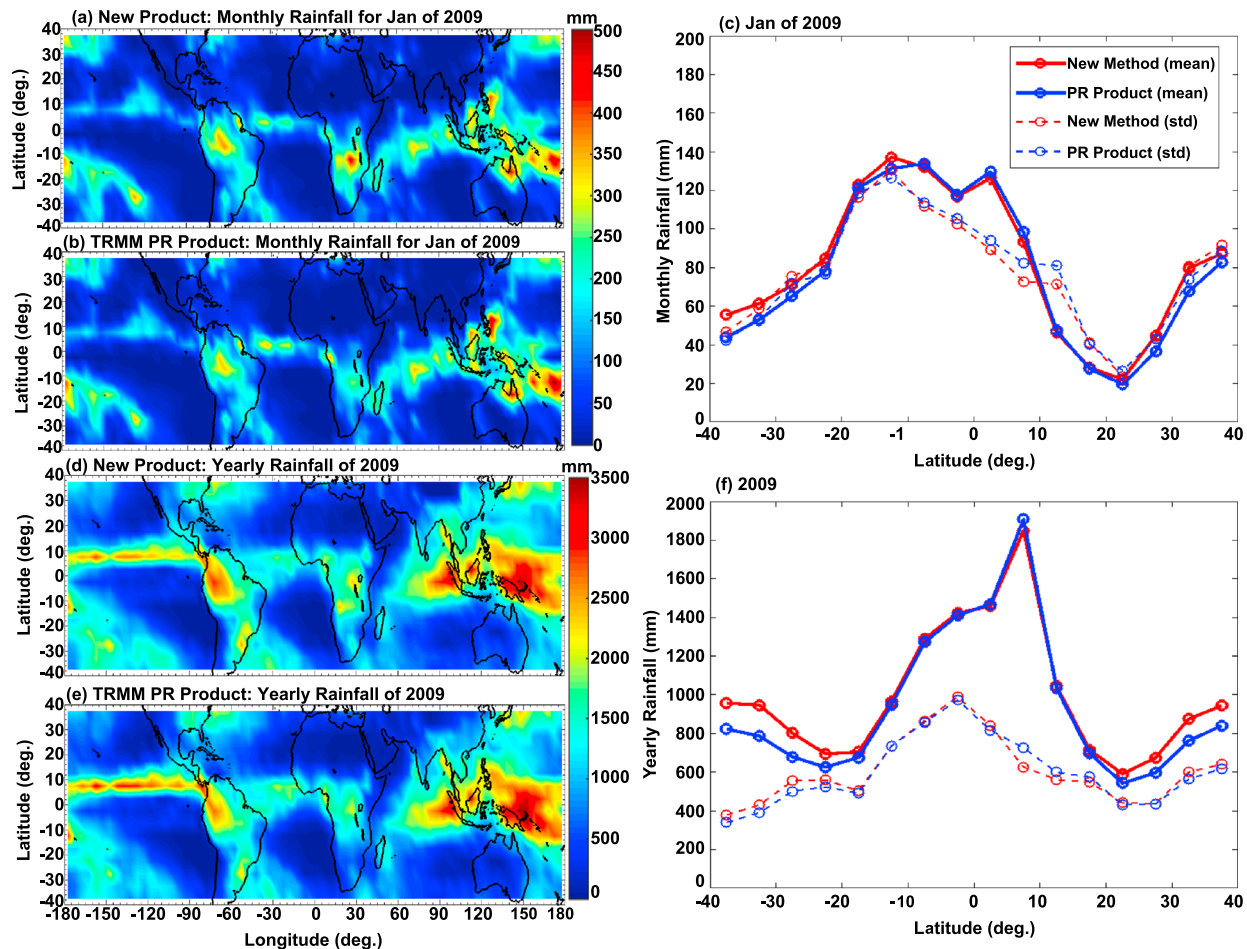
Figure 3. Sample monthly and yearly rainfall product for the region near Melbourne, FL, in 2009. Monthly rainfall map (May) derived using (a) the hybrid neural network system and (b) the standard Tropical Rainfall Measuring Mission (TRMM) Precipitation Radar (PR)product (i.e., 3A26); yearly rainfall derived using (d) the hybrid neural network system and (e) the standard TRMM PR product; (c) and (f) are the scatter plots of zonal means of rainfall estimates in (a) and (b) and (d) and (e), respectively.

where R_{Est} represents the estimated rainfall from the MLP-1 or MLP-2 model; R_{Ref} represents the reference rainfall from independent validation gauge or ground radar estimates or the standard TRMM PR products.

3. Results and Discussion

3.1. Quantification of Model Uncertainty

Figures 2a–2c illustrate a rainfall instance estimated by the ground-based KMLB radar and spaceborne PR during the satellite overpass at 0337UTC on 20 May 2009. In particular, the KMLB radar product in Figure 2a is derived using the MLP-1 model, whereas the PR estimates in Figure 2b are obtained from the MLP-2 model. The standard instantaneous rain rate product from TRMM program (Iguchi et al., 2000) corresponding to this time frame is shown in Figure 2c, for cross comparison. Overall, the three products exhibit similar pattern with a line of convection observed off the east coast of Florida and a region of more stratiform type rainfall over the peninsula. Scrutinizing Figures 2a–2c, it is also found that the PR precipitation estimates from the MLP-2 model is smoother and more realistic compared to the standard TRMM product,

Figure 4. Global rainfall products for the year 2009: Sample monthly rainfall map (January) derived using (a) the hybrid neural network system and (b) the standard Tropical Rainfall Measuring Mission (TRMM) Precipitation Radar (PR)product (i.e., 3A26); yearly rainfall derived using (d) the hybrid neural network system and (e) the standard TRMM PR product; (c) and (f) are the zonal means and standard deviations (std) of rainfall products illustrated in (a) and (b) and (d) and (e), respectively.

which is more scattered. In addition, the precipitation intensity estimated using the MLP-2 model agrees with the ground radar estimates better than the standard product does.

In order to further demonstrate the performance of the neural network models, we utilize the independent testing data to quantify the associated model uncertainties. Figures 2d and 2e, respectively, show the scatter plots of rainfall estimates from the MLP-1 and MLP-2 models versus the independent validation data sets. In Figure 2d, 6,516 data pairs (ground radar vs gauge) are included, while Figure 2e includes 586 sample pairs (PR vs ground radar). Obviously, both models exhibit good performance with low NMD and high CORR. The ground radar estimates from the MLP-1 model are highly correlated (0.95) with independent gauge measurements with a normalized bias of 1.4%. The correlation and normalized bias between PR estimates and independent ground radar products are 0.94 and 5.6%, respectively. Compared to previous studies, which use ground-based radar to validate the standard PR rainfall estimates (e.g., Kirstetter et al., 2012, 2014; Liao & Meneghini, 2009; Wolff et al., 2005), the scores in Figure 2e show superior performance of the MLP-2 model to the current algorithm adopted by the PMM program.

3.2. System Application and Verification

The other advantage of the proposed rainfall algorithm is that it is very flexible and can be easily applied to TRMM PR data after training. For illustration purpose, monthly rainfall maps are generated and compared to the standard PR products (i.e., TRMM 3A25 and 3A26) at both regional and global scales. The 3A25

Table 1
Cross Comparison Results Between Rainfall Estimates From the Proposed Hybrid Neural Network Approach and the Standard TRMM PR Products during 2009

	Regional product			Global product		
Year 2009	NMD (%)	NMAD (%)	CORR	NMD (%)	NMAD (%)	CORR
January	13.8	39.6	0.88	4.4	13.8	0.98
February	19.3	43.6	0.87	3.4	14.7	0.97
March	18.3	40.9	0.88	5.1	14.4	0.98
April	17.0	39.4	0.88	5.7	15.1	0.97
May	13.3	32.5	0.91	5.5	14.4	0.97
June	15.8	44.9	0.84	7.7	17.4	0.96
July	9.6	32.8	0.89	5.4	14.3	0.98
August	10.7	31.9	0.91	6.1	15.0	0.98
September	12.6	33.7	0.90	7.2	16.0	0.97
October	15.9	38.5	0.89	7.2	16.1	0.97
November	18.8	38.7	0.89	6.9	16.2	0.97
December	17.2	36.3	0.87	5.3	15.4	0.97
Monthly All	14.7	36.5	0.89	5.9	15.3	0.97
Yearly Total	12.7	20.3	0.93	5.8	10.8	0.98

Abbreviations: CORR, Pearson correlation coefficient; NMAD, normalized mean absolute difference; NMD, normalized mean difference; PR, Precipitation Radar; TRMM, Tropical Rainfall Measuring Mission.

product is produced on 0.5° × 0.5° latitude/longitude grid, whereas the 3A26 product is on 5° × 5° scale. Both are monthly products derived from PR 2A25 data. More details about how the 3A25 and 3A26 monthly rainfall maps are generated can be found from https://disc2.gesdisc.eosdis.nasa.gov/opendap/TRMM_L3/. For the high-resolution PR estimates from the MLP-2 model, at a certain pixel, the rainfall accumulation during a month is calculated by multiplying the mean rainfall rate within that pixel by the total number of hours in that month, and multiple grids are averaged in order to match the coarse resolution of standard TRMM product.

For regional analysis, a 10° × 10° area over the KMLB Florida region is considered. Figure 3 shows sample rainfall accumulation maps at 0.5° × 0.5° resolution for January and the whole year of 2009, including the scatter plots of corresponding zonal means of rainfall accumulation generated by the new approach versus the standard TRMM product. Results for other months are supplemented in Figure S1 in the supporting information. Although differences in the numerical values still exist, Figure 3 indicates that, on average, the rainfall maps generated by the MLP estimator are very similar to those derived from the standard TRMM product, demonstrating the feasibility of the proposed rainfall approach.

In order to explore the representativeness of this hybrid rainfall system, global monthly rainfall maps are also generated using the trained MLP-2 model. The global product is created pixel by pixel on 5° × 5° latitude/longitude grid to match the 3A26 product. Figure 4 shows example global rainfall products for January and the whole year of 2009, including both the standard 3A26 product and new product derived from the hybrid model, as well as the zonal means and standard deviations of these two products. Again, it can be seen that the products generated by the neural network estimator are very similar to the standard TRMM products at a global scale, which is further demonstrated by the scatter density plots in Figure S2. However, it is noted that the zonal means of the deep learning-based products are slightly higher at higher latitude than near the equator (20°N–20°S). This is likely because the regional model developed using Florida data can represent the precipitation features at lower latitudes better than middle latitudes.

Table 1 shows the numerical comparison results between the proposed hybrid model and standard PR product at both regional and global scales. It is concluded that the two products agree with each other fairly well, despite the PR product indicates slightly less precipitation with respect to the neural network product at both scales. The overall scores for 12 monthly rainfall combined have low NMD of 14.7% (5.9%) and high CORR of 0.89 (0.97) at regional (global) scale. In addition, the trained model using 2009 data is implemented for PR data collected during 2013 in order to further demonstrate its generic applicability. Results are supplemented in Table S1 and Figures S3–S6 in the supporting information, which essentially show similar performance to 2009.

3.3. Discussion

The closeness and behavior of rainfall indicated by the plots demonstrate that there is a good potential this nonparametric technique can be applied to spaceborne radar. The nonparametric scheme allows for adaptive relationships between PR reflectivity and rainfall compared to conventional "fixed" relations that may not adequately represent precipitation variability. Although exhaustive evaluation of such benefit in other regions characterized by different precipitation microphysics is still required, demonstration study in Florida shows that this machine learning approach could produce better estimates compared to the standard TRMM algorithm in regions where substantial gauge and radar data are available. It is also noteworthy that this hybrid system is very easy to implement. It can produce comparative estimates with the standard TRMM product if applied to other regions without changing the model, which is very appealing especially in the areas such as ocean and remote regions where no gauge or radar available. With more and more gauges and ground radars being deployed in the world and many of them become operational, this hybrid system can be trained at different locations with different atmosphere properties to further increase the dynamic adjustment and generality.

4. Summary

A nonparametric deep learning approach to rainfall estimation using TRMM PR measurements is described. Essentially, a two-stage deep neural network system was designed. The first was to map the relation between ground radar reflectivity and rainfall intensities from gauges. The second was to train spaceborne radar profiles using ground radar rainfall estimates. Data from 1 year of observations during 2009 in Florida were used to show the implementation of this innovative system. Validation using independent data in 2009 as well as 2-year comparison against the standard TRMM product demonstrated its promising performance. Although extensive application and evaluation for different precipitation types in different climate regions need to be conducted in future, this deep learning technique already showed the great potential for regional and global rainfall mapping.

In the GPM era, such machine learning-based approach should be considered in support of rainfall algorithm development for the dual-frequency precipitation radar, where the dual-frequency measurements should be suited to the MLP framework in order to better account for the precipitation microphysical variability. The approach proposed in this study will also provide insights into radar-radiometer combined precipitation estimates, which can serve as calibrator for the Integrated Multi-satellitE Retrievals for GPM (IMERG). In addition, this nonparametric system can be expanded as a data fusion platform through incorporating additional input features such as numerical weather prediction model results.

References

Bergstra, J. S., Bardenet, R., Bengio, Y., & Kegl, B. (2011). Algorithms for hyper-parameter optimization. *Proceedings of the 24th International Conference on Neural Information Processing Systems* (pp. 2546–2554).

Bolen, S., & Chandrasekar, V. (2003). Methodology for aligning and comparing spaceborne radar and ground-based radar observations. *Journal of Atmospheric and Oceanic Technology*, *20*(5), 647–659. https://doi.org/10.1175/1520-0426(2003)20<647:MFAACS>2.0.CO;2

Bringi, V. N., & Chandrasekar, V. (2001). *Polarimetric Doppler weather radar: Principles and applications* (p. 664). Cambridge, UK: Cambridge University Press. https://doi.org/10.1017/CBO9780511541094

Burges, C., Shaked, T., Renshaw, E., Lazier, A., Deeds, M., Hamilton, N., & Hullender, G. (2005). Learning to rank using gradient descent. *Proceedings of the 22nd International Conference on Machine Learning (ICML'05)*, 89-96. Bonn, Germany. https://doi.org/10.1145/1102351.1102363

Chen, H., Chandrasekar, V., & Bechini, R. (2017). An improved dual-polarization radar rainfall algorithm (DROPS2.0): Application in NASA IFloodS field campaign. *Journal of Hydrometeorology*, *18*(4), 917–937. https://doi.org/10.1175/JHM-D-16-0124.1

Cifelli, R., Chandrasekar, V., Chen, H., & Johnson, L. E. (2018). High resolution radar quantitative precipitation estimation in the San Francisco Bay Area: Rainfall monitoring for the urban environment. *Journal of the Meteorological Society of Japan*, *96A*(0), 141–155. https://doi.org/10.2151/jmsj.2018-016

Dolan, B., Fuchs, B., Rutledge, S. A., Barnes, E. A., & Thompson, E. J. (2018). Primary modes of global drop size distributions. *Journal of the Atmospheric Sciences*, *75*(5), 1453–1476. https://doi.org/10.1175/JAS-D-17-0242.1

Gou, Y., Ma, Y., Chen, H., & Wen, Y. (2018). Radar-derived quantitative precipitation estimation in complex terrain over the eastern Tibetan Plateau. *Atmospheric Research*, *203*, 286–297. https://doi.org/10.1016/j.atmosres.2017.12.017

Hinton, G. E., & Salakhutdinov, R. R. (2006). Reducing the dimensionality of data with neural networks. *Science*, *313*, 504–507. https://doi.org/10.1126/science.1127647

Iguchi, T., Kozu, T., Meneghini, R., Awaka, J., & Okamoto, K. (2000). Rain-profiling algorithm for the TRMM precipitation radar. *Journal of Applied Meteorology and Climatology*, *39*(12), 2038–2052. https://doi.org/10.1175/1520-0450(2001)040<2038:RPAFTT>2.0.CO;2

Kirstetter, P. E., Gourley, J. J., Hong, Y., Zhang, J., Moazamigoodarzi, S., Langston, C., & Arthur, A. (2015). Probabilistic precipitation rate estimates with ground-based radar networks. *Water Resources Research*, *51*, 1422–1442. https://doi.org/10.1002/2014WR015672

Kirstetter, P. E., Hong, Y., Gourley, J. J., Cao, Q., Schwaller, M., & Petersen, W. (2014). Research framework to bridge from the global precipitation measurement mission core satellite to the constellation sensors using ground-radar-based national mosaic QPE. In V. Lakshmi, D. Alsdorf, M. Anderson, S. Biancamaria, M. Cosh, J. Entin, G. Huffman, W. Kustas, P. van Oevelen, T. Painter, J. Parajka, M. Rodell, & C. Rüdiger (Eds.), *Remote Sensing of the Terrestrial Water Cycle* (Chap. 4, pp. 61–79). Hoboken, NJ: John Wiley & Sons, Inc. https://doi.org/10.1002/9781118872086.ch4

Kirstetter, P. E., Hong, Y., Gourley, J. J., Chen, S., Flamig, Z., Zhang, J., et al. (2012). Toward a framework for systematic error modeling of spaceborne precipitation radar with NOAA/NSSL ground radar-based national mosaic QPE. *Journal of Hydrometeorology*, *13*(4), 1285–1300. https://doi.org/10.1175/JHM-D-11-0139.1

Kitchen, M., Brown, R., & Davies, A. (1994). Real-time correction of weather radar data for the effects of bright band, range and orographic growth in widespread precipitation. *Quarterly Journal of the Royal Meteorological Society*, *120*(519), 1231–1254. https://doi.org/10.1002/qj.49712051906

Kozu, T., Kawanishi, T., Kuroiwa, H., Kojima, M., Oikawa, K., Kumagai, H., et al. (2001). Development of precipitation radar onboard the Tropical Rainfall Measuring Mission (TRMM) satellite. *IEEE Transactions on Geoscience and Remote Sensing*, *39*(1), 102–116. https://doi.org/10.1109/36.898669

Kummerow, C., Barnes, W., Kozu, T., Shiue, J., & Simpson, J. (1998). The Tropical Rainfall Measuring Mission (TRMM) sensor package. *Journal of Atmospheric and Oceanic Technology*, *15*(3), 809–817. https://doi.org/10.1175/1520-0426(1998)015<0809:TTRMMT>2.0.CO;2

LeCun, Y., Bengio, Y., & Hinton, G. (2015). Deep learning. *Nature*, *521*(7553), 436–444. https://doi.org/10.1038/nature14539

Liao, L., & Meneghini, R. (2009). Validation of TRMM precipitation radar through comparison of its multiyear measurements with ground-based radar. *Journal of Applied Meteorology and Climatology*, *48*(4), 804–817. https://doi.org/10.1175/2008JAMC1974.1

Liu, H., Chandrasekar, V., & Xu, G. (2001). An adaptive neural network scheme for radar rainfall estimation from WSR-88D observations. *Journal of Applied Meteorology*, *40*(11), 2038–2050. https://doi.org/10.1175/1520-0450(2001)040<2038:AANNSF>2.0.CO;2

Orlandini, S., & Morlini, I. (2000). Artificial neural network estimation of rainfall intensity from radar observations. *Journal of Geophysical Research*, *105*(D20), 24,849–24,861. https://doi.org/10.1029/2000JD900408

Schwaller, M. R., & Morris, K. R. (2011). A ground validation network for the Global Precipitation Measurement mission. *Journal of Atmospheric and Oceanic Technology*, *28*(3), 301–319. https://doi.org/10.1175/2010JTECHA1403.1

Steiner, M., & Smith, J. A. (2000). Reflectivity, rain rate, and kinetic energy flux relationships based on raindrop spectra. *Journal of Applied Meteorology*, *39*(11), 1923–1940. https://doi.org/10.1175/1520-0450(2000)039<1923:RRRAKE>2.0.CO;2

Tan, H., Chandrasekar, V., & Chen, H. (2017). A machine learning model for radar rainfall estimation based on gauge observations. *United States National Committee of URSI National Radio Science Meeting (USNC-URSI NRSM)*, Boulder, CO, 1-2.

Teschl, R., Randeu, W. L., & Teschl, F. (2007). Improving weather radar estimates of rainfall using feed-forward neural networks. *Neural Networks*, *20*(4), 519–527. https://doi.org/10.1016/j.neunet.2007.04.005

Wen, G., Chen, H., Zhang, G., & Sun, J. (2018). An inverse model for raindrop size distribution retrieval with polarimetric variables. *Remote Sensing*, *10*(8), 1179. https://doi.org/10.3390/rs10081179

Wolff, D. B., Marks, D. A., Amitai, E., Silberstein, D. S., Fisher, B. L., Tokay, A., et al. (2005). Ground validation for the Tropical Rainfall Measuring Mission (TRMM). *Journal of Atmospheric and Oceanic Technology*, *22*(4), 365–380. https://doi.org/10.1175/JTECH1700.1

Xiao, R., & Chandrasekar, V. (1997). Development of a neural network based algorithm for rainfall estimation from radar observations. *IEEE Transactions on Geoscience and Remote Sensing*, *35*(1), 160–171. https://doi.org/10.1109/36.551944

Xu, G., & Chandrasekar, V. (2005). Operational feasibility of neural-network-based radar rainfall estimation. *IEEE Geoscience and Remote Sensing Letters*, *2*(1), 13–17. https://doi.org/10.1109/LGRS.2004.842338